Modelling of Progress Variable Variance Transport in Head on Quenching of Turbulent Premixed Flames: A Direct Numerical Simulation Analysis

Jiawei Lai[1], Nilanjan Chakraborty[1]
[1]School of Mechanical and Systems Engineering, Newcastle University
Newcastle-Upon-Tyne, Tyne and Wear, NE1 7RU, United Kingdom

1 Introduction

In turbulent premixed combustion the reactive scalar field is often characterized with the help of a reaction progress variable c, which can be defined in terms of a suitable reactant mass fraction Y_R in such a manner that $c = (Y_{R0} - Y_R)/(Y_{R0} - Y_{R\infty})$ increases monotonically from zero in unburned gas (subscript 0) to unity in fully burned products (subscript ∞). The variance of reaction progress variable $\widetilde{c''^2}$ (where the Favre average and Favre fluctuation of a general quantity q are $\tilde{q} = \overline{\rho q}/\bar{\rho}$ and $q'' = q - \tilde{q}$ respectively, with ρ being the gas density and the over-bar indicating a Reynold averaging operation) is one of the important quantities for the flamelet and conditional moment based closures [1]. According to Bray-Moss-Libby (BML) modelling [2] $\widetilde{c''^2}$ can be expressed as: $\widetilde{c''^2} = \tilde{c}(1-\tilde{c}) + O(\gamma_c)$ where $O(\gamma_c)$ is the burning mode probability density function (pdf) contribution. The contribution of $O(\gamma_c)$ can be neglected and $\widetilde{c''^2}$ assumes its maximum possible value $\tilde{c}(1-\tilde{c})$ when the pdf of c can be approximated by a bi-modal distribution with impulses at $c = 0$ and 1.0. This assumption is strictly valid for high values of Damköhler number (i.e. $Da \gg 1$) but $O(\gamma_c)$ cannot be neglected for small values of Da (i.e. $Da < 1$) and subsequently $\widetilde{c''^2}$ remains smaller than $\tilde{c}(1-\tilde{c})$. Thus, it may be necessary to solve a transport equation for $\widetilde{c''^2}$ along with other modelled conservation equations in the context of Reynolds Averaged Navier Stokes (RANS) simulations of low Damköhler number (i.e. $Da < 1$) combustion. The transport of $\widetilde{c''^2}$ in the near-wall region for head on quenching of turbulent premixed flames has not been analysed in the existing literature. This gap has been addressed here by carrying out three-dimensional Direct Numerical Simulations (DNS) of head on quenching of statistically planar turbulent premixed flames for different values of turbulent Reynolds number Re_t and global Lewis number $Le = \lambda/(\rho C_P D)$ where α_T, λ, C_P and D are the thermal conductivity, specific heat at constant pressure and mass diffusivity respectively.

2 Mathematical Background and Numerical Implementation

The transport equation of $\widetilde{c''^2}$ takes the following form [1,2]:

$$\frac{\partial(\bar{\rho}\widetilde{c''^2})}{\partial t} + \frac{\partial(\bar{\rho}\tilde{u}_j\widetilde{c''^2})}{\partial x_j} = \underbrace{\frac{\partial}{\partial x_j}\left[\rho D \frac{\partial \widetilde{c''^2}}{\partial x_j}\right]}_{D_{1c}} \underbrace{- \frac{\partial\left(\overline{\rho u_j'' c''^2}\right)}{\partial x_j}}_{T_{1c}} \underbrace{- 2\overline{\rho u_j'' c''} \frac{\partial \tilde{c}}{\partial x_j}}_{T_{2c}} + \underbrace{2(\overline{\dot{\omega} c} - \bar{\dot{\omega}}\tilde{c})}_{T_{3c}} - \underbrace{2\bar{\rho}\tilde{\varepsilon}_c}_{D_{2c}} \qquad (1)$$

Correspondence to: j.lai@newcastle.ac.uk

where $\dot{\omega}$ and $\widetilde{\varepsilon_c} = \overline{\rho D \nabla c'' \cdot \nabla c''}\,/\bar{\rho}$ are the reaction rate and the scalar dissipation rate (SDR) of c respectively. In Eq. 1, D_{1c} is a closed term which denotes the molecular diffusion of $\widetilde{c''^2}$, T_{1c} is the turbulent transport term, T_{2c} represents generation/destruction of $\widetilde{c''^2}$ by the mean scalar gradient, T_{3c} is the reaction rate contribution and $(-D_{2c})$ is the molecular dissipation term. The term T_{2c} is closed in the context of second-moment closure, so the terms T_{1c}, T_{3c} and $(-D_{2c})$ are the unclosed term in the context of $\widetilde{c''^2}$ closure. Equation 1 indicates that $(-D_{2c})$ closure translates to the modelling of $\tilde{\varepsilon}_c$. The modelling of T_{1c}, T_{3c} and $\tilde{\varepsilon}_c$ for the head on quenching of premixed turbulent combustion has been investigated here using explicitly Reynolds averaging three-dimensional DNS data.

The chemical mechanism is simplified using a single step chemical reaction (i.e. $Reactants \rightarrow Products$) for the present analysis, as three-dimensional DNS simulations with detailed chemistry are still too expensive to carry out an extensive parametric analysis. Furthermore, simple chemistry DNS allows for the investigation of the influences of global Lewis number on $\widetilde{c''^2}$ transport in isolation. Here, the conservation equations of mass, momentum, energy and species for compressible reacting flows are solved in non-dimensional using a well-known DNS code SENGA [1]. The simulation domain is taken to be a rectangular box of size $70.6\delta_Z \times 35.2\delta_Z \times 35.2\delta_Z$, where $\delta_Z = \alpha_{T0}/S_L$ is Zel'dovich flame thickness with α_{T0} and S_L being the thermal diffusivity of unburned gas and unstrained laminar burning velocity respectively. The simulation domain is discretized using a Cartesian grid of $512 \times 256 \times 256$ ensuring 10 grid points across the thermal flame thickness $\delta_{th} = (T_{ad} - T_0)/Max\left|\nabla \hat{T}\right|_L$ where $\hat{T}$, T_0 and T_{ad} are the instantaneous, unburned gas and adiabatic flame temperatures respectively, and the subscript 'L' is used to refer to the unstrained laminar flame quantities. The left hand side boundary in the x_1 direction (i.e. $x_1 = 0$) is taken to be no-slip wall with temperature $T_w = T_0$ and zero mass flux is imposed in the wall normal direction. Partially non-reflecting outlet boundary condition is specified in the right hand side boundary in the x_1 direction. Transverse directions are considered to be periodic. The Reynolds averaging is carried out by ensemble averaging the quantities over statistically homogeneous $x_2 - x_3$ directions at a given x_1 location. Three different global Lewis numbers (0.8, 1.0 and 1.2) have been considered for this analysis and standard values are chosen for Zel'dovich number (i.e. $\beta = T_{ac}\,(T_{ad} - T_0)/T_{ad}^2 = 6$), Prandtl number (i.e.$Pr = 0.7$) and the ratio of specific heats (i.e. $\gamma = 1.4$) where T_{ac} is the activation temperature. The heat release parameter $\tau = (T_{ad} - T_0)/T_0$ is taken to be 6.0 for all cases considered here. The simulations have been carried out for three different initial values of normalized root mean square value of turbulent velocity u'/S_L, Damköhler number $Da = lS_L/\delta_{th}u$, Karlovitz number $Ka = (u'/S_L)^{3/2}/(l/\delta_{th})^{-1/2}$ and turbulent Reynolds number $Re_t = \rho_0 u' l/\mu_0$, which are listed in Table 1 where ρ_0 and μ_0 are the unburned gas density and viscosity respectively.

Table 1: List of initial non-dimensional simulation parameters

Case	u'/S_L	l/δ_{th}	Re_t	Da	Ka
A	7.5	2.5	49.0	0.33	13.0
B	9.0	4.31	100.0	0.48	13.0
C	11.25	3.75	110.0	0.33	19.5

3 Results and Discussion

The non-dimensional temperature $T = (\hat{T} - T_0)/(T_{ad} - T_0)$ field in the central $x_1 - x_2$ plane for the turbulent case C is shown Fig. 1a. It can be seen from Fig. 1a that for the unity Lewis number case, c and T are identical when the flame is away from wall (e.g. $t = \delta_Z/S_L$), which is not the case for the $Le = 0.8$ and 1.2 cases but these two quantities become significantly different from each other in the near-wall region once the quenching starts. The temporal evolutions of normalised wall heat flux $\Phi = |q_w|/[\rho_0 S_L C_P (T_{ad} - T_0)]$ and wall Peclet number $Pe = X/\delta_Z$ (where X is the wall normal distance of

$T = 0.9$ iso-surface) for both laminar and turbulent conditions are also shown in Fig. 1 for case C. For the laminar case Φ (Pe) increases (decreases) as the flame approaches the wall and Φ and Pe assume the maximum and minimum values respectively when the flame quenches (see Fig. 1b). The same behaviour has been observed for mean values of Φ and Pe in the turbulent cases and the minimum value of wall Peclet number (i.e. Pe_{min}) remains comparable to the corresponding laminar flame value $(Pe_{min})_L$. However, the maximum value of Φ in the turbulent case assumes greater magnitude than the corresponding laminar value, and the maximum heat flux for the turbulent $Le = 0.8$ flame has been found to be greater than in the turbulent $Le = 1.0$ and 1.2 flames. The variations of $\widetilde{c''^2}$ and $\bar{\dot{\omega}}$ in the direction normal to the wall are shown in Fig. 2 for different time instants. Figure 2 reveals that no reaction takes place in where $x_1/\delta_Z < (Pe_{min})_L$ due to large heat loss through the wall. It can be seen from Fig. 2 that $\widetilde{c''^2}$ remains smaller than $\tilde{c}(1-\tilde{c})$ in all cases due to $Da < 1$. A comparison between $\widetilde{c''^2}$ and $\bar{\dot{\omega}}$ variations indicates that $\widetilde{c''^2}$ drops significantly during flame quenching and eventually vanishes even when $\tilde{c}(1-\tilde{c})$ assumes non-zero values (i.e. $\tilde{c}(1-\tilde{c}) \neq 0$). The difference between $\tilde{c}(1-\tilde{c})$ and $\widetilde{c''^2}$ provides the extent of departure of $P(c)$ from a perfect bi-modal distribution with impulses at $c = 0$ and 1.0. The results in Fig. 2 indicate that $P(c)$ deviates significantly from a bi-modal distribution in the near-wall region [7].

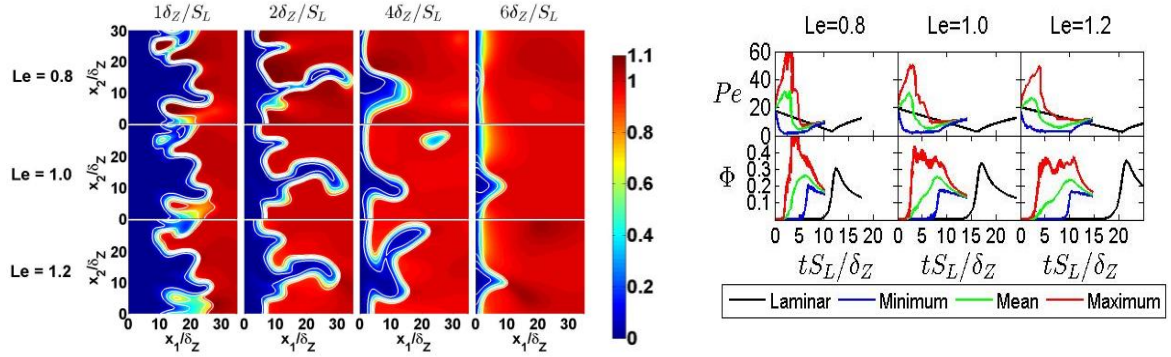

(a) (b)

Figure 1. (a) Distributions of T contours for turbulent case C at t= $1\delta_Z/S_L$ - $6\delta_Z/S_L$. The contours of c from 0.1 to 0.9 in steps of 0.2 (from left to right) are shown by white lines. (b) Temporal evolution of wall Peclet number Pe and normalised wall heat flux Φ for turbulent case C.

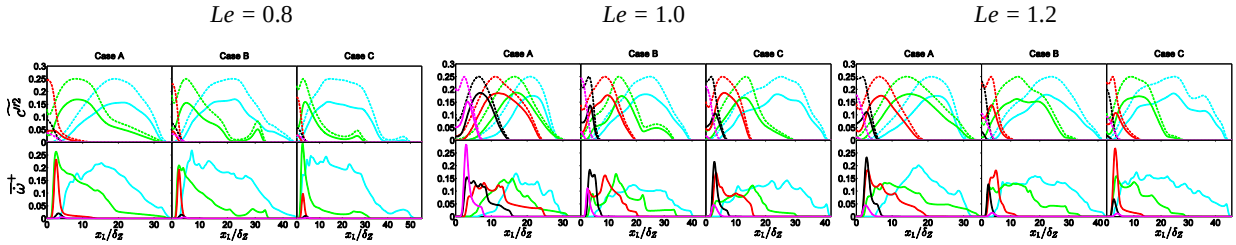

Figure 2. Variation of $\widetilde{c''^2}$ (solid line), $\tilde{c}(1-\tilde{c})$ (broken line) (shown in top row) and $\bar{\dot{\omega}}^+ = \bar{\dot{\omega}} \times \delta_Z/\rho_0 S_L$ (shown in in bottom row) with x_1/δ_Z at t = —2 δ_Z/S_L; — $4\delta_Z/S_L$; — $6\delta_Z/S_L$; — $8\delta_Z/S_L$; — $10\delta_Z/S_L$ for cases A-C for Le=0.8, 1.0 and 1.2.

The variations of $D_{1c}, T_{1c}, T_{2c}, T_{3c}$ and $(-D_{2c})$ with x_1/δ_Z are shown in Fig. 3 for all cases considered here. For all cases T_{3c} and $(-D_{2c})$ remain leading order source and sink terms respectively when the flame is away from the wall. The turbulent scalar flux $\overline{\rho u_1'' c''}$ shows counter-gradient transport for all cases considered here which leads to negative value of T_{2c}. The turbulent transport term T_{1c} shows negative values close to the wall but assumes positive values away from wall. The relative magnitude of D_{1c} in comparison to the other terms decreases with increasing Re_t . A comparison between Figs. 2 and 3 shows that the magnitude of all terms in $\widetilde{c''^2}$ transport equation decays significantly in the near-wall region where the flame quenching takes place. Modelling of T_{1c} requires the modelling of

$\overline{\rho u_i'' \, c''^2}$ and this translates to the modelling of $\overline{\rho u_1'' \, c''^2}$ for statistical planar flames. Chakraborty and Swaminathan [1] proposed the following model for $\overline{\rho u_1'' \, c''^2}$:

$$\overline{\rho u_1'' \, c''^2} = \overline{\rho u_1'' \, c''} \cdot \left\{1 - 2\tilde{c} \cdot \left[\widetilde{c''^2}/\left(\tilde{c} \cdot (1-\tilde{c})\right)\right]^{0.3}\right\} \cdot 2\widetilde{c''^2}/\left[\widetilde{c''^2} + \tilde{c} \cdot (1-\tilde{c})\right] \quad (2)$$

Figure 4 shows that Eq. 2 mostly provides satisfactory performance away from the wall but this model underpredicts the extent of negative contribution of $\overline{\rho u_1'' \, c''^2}$ close to the wall. It has been found that the following modification yields better agreement with $\overline{\rho u_1'' \, c''^2}$ extracted from DNS data:

$$\overline{\rho u_1'' \, c''^2} = \overline{\rho u_1'' \, c''} \cdot \left\{A_w^3 - 2\tilde{c} \cdot \left[\widetilde{c''^2}/\left(\tilde{c} \cdot (1-\tilde{c})\right)\right]^{0.3}\right\} \cdot 2\widetilde{c''^2}/\left[\widetilde{c''^2} + \tilde{c} \cdot (1-\tilde{c})\right] \quad (3)$$

where $A_w = -\mathrm{e}^{Le(\tilde{c}-\tilde{T})} + 2$ and this term remains active close to the wall where $\tilde{c} \neq \tilde{T}$ but A_w asymptotically approaches 1.0 away from the wall and thus Eq. 3 reduces to Eq. 2 away from the wall.

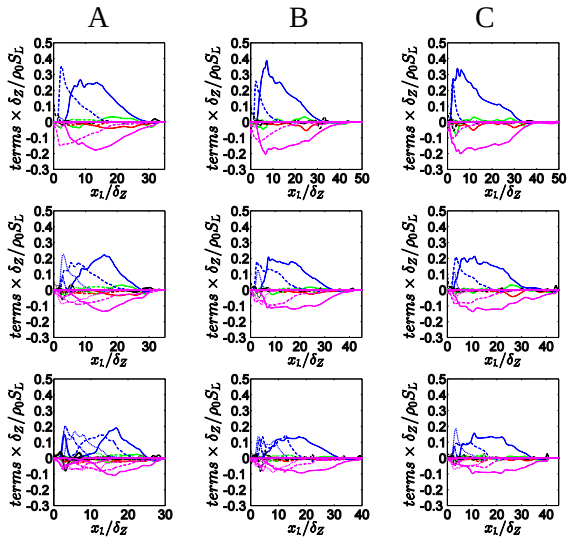

——, $\delta_Z/S_L = 2$; -----, $\delta_Z/S_L = 4$; ·····, $\delta_Z/S_L = 6$; – · – ·, $\delta_Z/S_L = 8$; ——, $\delta_Z/S_L = 10$;

Figure 3. Variations of the terms ——, T_{1c}; ——, T_{2c}; ——, T_{3c}; ——, D_{1c} and ——, $(-D_{2c})$ with x_1/δ_Z at t = 2, 4, 6, 8 and 10 δ_Z/S_L for cases A-C for Le = 0.8 (1st row), 1.0 (2nd row) and 1.2 (3rd row).

According to Bray [2] the T_{3c} can be modelled as: $T_{3c} = 2\bar{\dot{\omega}}(c_m - \tilde{c})$ with $c_m = \int_0^1 [\dot{\omega}\, c f(c)]_L dc \,/\, \int_0^1 [\dot{\omega}\, f(c)]_L dc$ where $f(c)$ is the burning mode pdf. The mean reaction rate $\bar{\dot{\omega}}$ can be modelled as: $\bar{\dot{\omega}} = 2\bar{\rho}\widetilde{\varepsilon_c}/(2c_m - 1)$ [2] for $Da \gg 1$ flames where $P(c)$ can be approximated by a bi-modal distribution. Thus, the reaction rate term T_{3c} can be expressed as: $T_{3c} = [4\bar{\rho}\widetilde{\varepsilon_c}(c_m - \tilde{c})]/(2c_m - 1)$ according to Bray [2]. It can be seen from Fig. 4 that $[4\bar{\rho}\widetilde{\varepsilon_c}(c_m - \tilde{c})]/(2c_m - 1)$ satisfactorily predicts T_{3c} when the flame is away from wall but once the quenching starts, $[4\bar{\rho}\widetilde{\varepsilon_c}(c_m - \tilde{c})]/(2c_m - 1)$ shows non-zero value at wall and in the near wall region, where T_{3c} either vanishes or assumes negligible values. This behaviour originates due to non-zero value of $2\bar{\rho}\widetilde{\varepsilon_c}/(2c_m - 1)$ in the near wall region where $\bar{\dot{\omega}}$ is zero due to flame quenching (not shown here). This discrepancy between $\bar{\dot{\omega}}$ and $2\bar{\rho}\widetilde{\varepsilon_c}/(2c_m - 1)$ originates due to non bi-modal pdf of c in the near wall region (see the differences between $\tilde{c}(1-\tilde{c})$ and $\widetilde{c''^2}$ in Fig. 2). It has been demonstrated in previous analyses [3-6] that $\bar{\dot{\omega}} = \rho_0 S_L \Sigma_{gen}$ (where $\Sigma_{gen} = |\overline{\nabla c}|$ is the generalised Flame Surface Density (FSD)) overestimates $\bar{\dot{\omega}}$ in the near wall region where the quenching takes place for flames with $Le = 1.0$ [3-6]. For $Le = 1.0$ flames $\rho_0 S_L \Sigma_{gen}$ accurately predicts $\bar{\dot{\omega}}$ away from the wall but $\rho_0 S_L \Sigma_{gen}$ underpredicts (overpredicts) $\bar{\dot{\omega}}$ for the $Le = 0.8$ ($Le = 1.2$) cases even when the flame is away from the wall [8]. By contrast, $2\bar{\rho}\widetilde{\varepsilon_c}/(2c_m - 1)$ predicts $\bar{\dot{\omega}}$ satisfactorily for all cases irrespective of Le when the flame away from the wall (i.e. before the initiation of flame quenching)

[7,8]. Here, the aforementioned behaviours of SDR (FSD) based closures in the near wall region have been utilised to propose the following model for T_{3c}:

$$T_{3c} = 2\left[\frac{2\bar{\rho}\widetilde{\varepsilon_c}}{2c_m-1}A_1 e^{Le(\tilde{c}-\tilde{T})} + A_2A_3\frac{\rho_0 S_L}{Le^B}\sqrt{\frac{\widetilde{\varepsilon_c}}{\tilde{D}}}\,e^{-0.5\left(\frac{x_1}{\delta_Z}-\theta\right)^2}\right](c_m-\tilde{c}) \qquad (4)$$

where $\theta = (Pe_{min})_L[\mathrm{erf}(8Le-6.0)+1]/2$. For the present thermo-chemistry $(Pe_{min})_L$ is found to be 3.09, 2.83 and 2.75 for the $Le = 0.8$, 1.0 and 1.2 cases respectively. In Eq. 4, $A_1 = 0.5\{erf[3.0(x_1/\delta_Z-\theta)]+1\}$, $A_2 = 0.5[erf(x_1/\delta_Z-\theta)+1]$, $A_3 = 2.31erf\left[2.6\left(\tilde{c}-\tilde{T}\right)\right]$ and $B = -6(Le-1)$ are the model parameters. Equation 4 reduces to $[4\bar{\rho}\widetilde{\varepsilon_c}(c_m-\tilde{c})]/(2c_m-1)$ away from the wall where $A_1e^{Le(\tilde{c}-\tilde{T})} = 0$ and $A_2A_3 = 0$. The involvement of $1/Le^B$ in the second term on right hand side of Eq. 4 compensates for the underprediction (overprediction) of $\bar{\omega}$ by $\rho_0 S_L\Sigma_{gen}\sim\rho_0 S_L\sqrt{\widetilde{\varepsilon_c}/\tilde{D}}$ for the turbulent $Le<1$ ($Le>1$) cases. Figure 4 shows that Eq. 4 satisfactorily predicts T_{3c} for all cases considered here

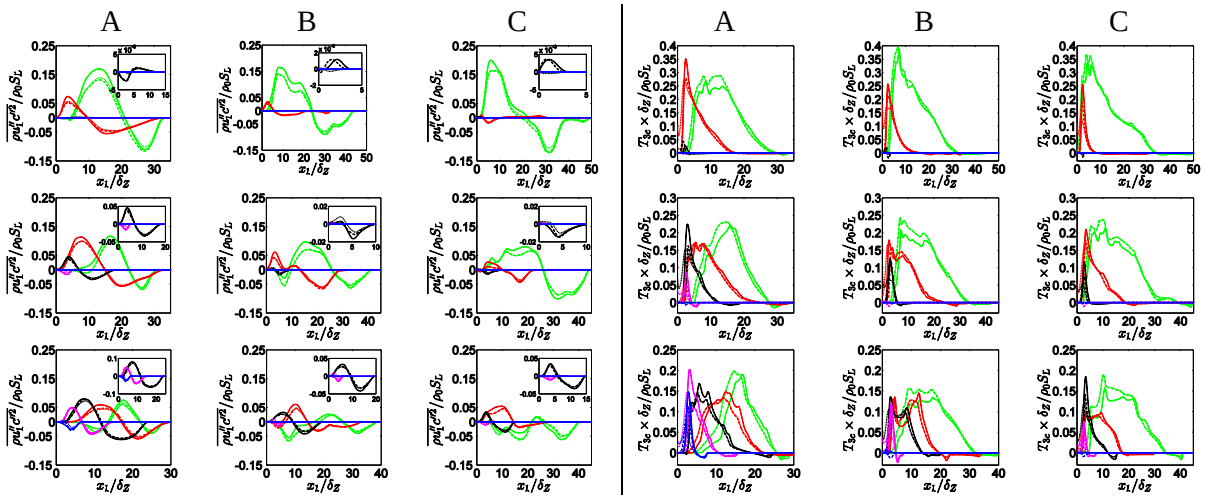

Figure 4. Variations of $\overline{\rho u_1'' c''^2}$ (1st column) and T_{3c} (2nd column) extracted from DNS data (solid line) and the predictions of Eqs. 2 (dash-dotted line) and 3 (thick broken line) (1st column), and $[4\bar{\rho}\widetilde{\varepsilon_c}(c_m-\tilde{c})]/(2c_m-1)$ (dash-dotted line) and Eq. 4 (thick broken line) with x_1/δ_Z at t = — $2\delta_Z/S_L$; — $4\delta_Z/S_L$; — $6\delta_Z/S_L$; — $8\delta_Z/S_L$; — $10\delta_Z/S_L$, for cases A-C and Le = 0.8 (1st row), 1.0 (2nd row) and 1.2 (3rd row).

The SDR $\widetilde{\varepsilon_c}$ needs to be modelled in order to model D_{2c} as well as for the modelling T_{3c} using Eq. 4. Chakraborty and Swaminathan [1] proposed an algebraic SDR $\widetilde{\varepsilon_c}$ model as:

$$\widetilde{\varepsilon_c} = \frac{1}{\beta'}\left(2\frac{K_c^*}{Le^{1.88}}\frac{S_L}{\delta_{th}} + C_3\frac{\tilde{\varepsilon}}{\tilde{k}} - \tau\frac{C_4(1-\tilde{c})^{\Phi}}{Le^{2.57}}\frac{S_L}{\delta_{th}}\right)\tilde{c}\,(1-\tilde{c}) \qquad (5)$$

where the thermo-chemical paramerter $K_c^* = \int_0^1[\rho(D\nabla c\cdot\nabla c)\nabla\cdot\vec{u}f(c)]_L dc/\int_0^1[\rho(D\nabla c\cdot\nabla c)f(c)]_L dc$ is equal to 0.74τ, 0.78τ and 0.80τ for $Le = 0.8$, 1.0 and 1.2 respectively, $\beta' = 6.7$, $\Phi = 0.2+1.5(1-Le)$, $C_3 = 2\sqrt{Ka_L}/(1+\sqrt{Ka_L})$ and $C_4 = 1.2/(1+Ka_L)^{0.4}$ are the model parameters [1] and $Ka_L = (\delta_{th}\tilde{\varepsilon}/S_L^3)^{1/2}$ is the local Karlovitz number with $\tilde{\varepsilon}$ being the dissipation rate of turbulent kinetic engery $\tilde{k}$. Figure 5 shows that Eq. 5 significanly overpredicts $\tilde{\varepsilon}_c$ in the near wall region where the flame quenching takes place. Here Eq. 5 has been modified in the following manner:

$$\widetilde{\varepsilon_c} = \frac{A_\epsilon e^{-1.2Le(\tilde{c}_w-\tilde{T}_w)^3}}{\beta'}\left(2\frac{K_c^*}{Le^{1.88}}\frac{S_L}{\delta_{th}} + C_3\frac{\tilde{\varepsilon}}{\tilde{k}} - \tau\frac{C_4(1-\tilde{c})^{\Phi}}{Le^{2.57}}\frac{S_L}{\delta_{th}}\right)\tilde{c}\,(1-\tilde{c}) \qquad (6)$$

where $\tilde{Q}_W$ is the Favre mean value at the wall for a genral quantity Q at a given instant of time. The parameters $A_\epsilon = 0.5[\mathrm{erf}(x_1/\delta_Z-\theta)+1]$and $e^{-1.2Le(\tilde{c}_w-\tilde{T}_w)^3}$ asymptotically approach 1.0 away from the wall. Figure 5 shows that Eq. 6 predicts $\widetilde{\varepsilon_c}$ accurately for both near to and away from the wall.

4 Conclusions

The near-wall transport of $\widetilde{c''^2}$ in the case of head on quenching of turbulent premixed flames has been analysed here using three-dimensional DNS data of statistically planar flames with *Le* is ranging from 0.8 to 1.2 for different values of Re_t. It has been found that the existing models for the turbulent transport, reaction and dissipation contributions (i.e. T_{1c}, T_{3c} and $-D_{2c}$) to the variance $\widetilde{c''^2}$ transport do not adequately capture the near-wall behaviour. Here the existing models for T_{1c}, T_{3c} and $-D_{2c}$ have been modified in order to account for the near-wall $\widetilde{c''^2}$ transport and the predictions of these modified models have been found to be satisfactory both near to and away from the wall.

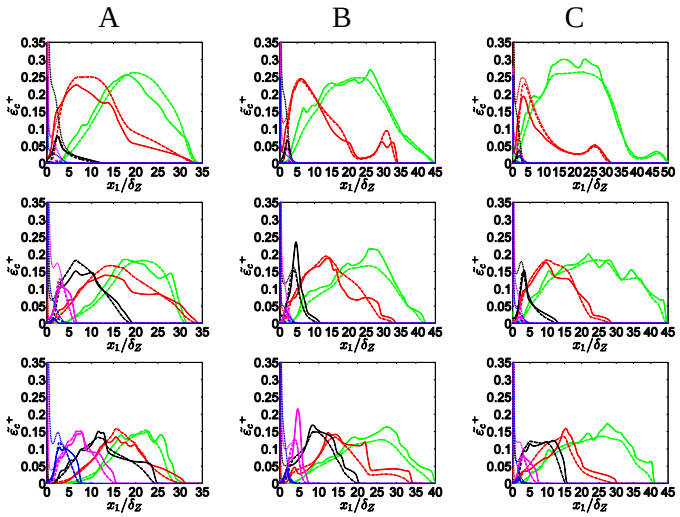

Figure 5. Variation of $\tilde{\varepsilon}_c^+ = \widetilde{\varepsilon_c} \times \delta_Z/S_L$ (solid line) and the predictions of Eq. 5 (dash-dotted line) and Eq. 6 (thick broken line) with x_1/δ_Z at t = — $2\delta_Z/S_L$; — $4\delta_Z/S_L$; — $6\delta_Z/S_L$; — $8\delta_Z/S_L$; — $10\delta_Z/S_L$, for case A-C and Lewis number *Le* = 0.8 (1st row), *Le* = 1.0 (2nd row) and *Le* = 1.2 (3rd row).

References

[1] Chakraborty N, Swaminathan N. (2010). Effects of Lewis number on scalar variance transport in premixed flames. Flow Turb. Combust. 87: 261.

[2] Bray K.N.C, Libby P.A., Moss, J.B. (1985). Unified modelling approach for premixed turbulent combustion-Part I: general formulation. Combust. Flame. 61:87.

[3] Poinsot TJ, Haworth DC, Bruneaux G. (1993). Direct simulation and modeling of flame-wall interaction for premixed turbulent combustion. Combust. Flame. 95: 118.

[4] Bruneaux G, Poinsot TJ, Ferziger J.H. (1997). Premixed flame-wall interaction in a turbulent channel flow: budget for the flame surface density evolution equation and modelling. J. Fluid Mech. 349: 191.

[5] Alshaalan T, Rutland CJ. (1998) Turbulence, scalar transport, and reaction rates in flame-wall interaction, Proc. Combust. Inst., 27:793.

[6] Gruber A, Sankaran R, Hawkes ER, Chen JH. (2010). Turbulent flame-wall interaction: a direct numerical simulation study. J. Fluid Mech. 658: 5.

[7] Lai, J., Chakraborty, N. (2014) Effects of Lewis number on head on quenching of turbulent premixed flame: A Direct Numerical Simulation analysis, Proc. SPEIC2014-Towards sustainable combustion, Lisboa, Portugal, 19th -21st November, 2014.

[8] Chakraborty N., Cant R.S. (2011). Effects of Lewis number on Flame Surface Density transport in turbulent premixed combustion", Combust. Flame, 158: 1768.